Reactive Power Constrained OPF Scheduling With 2-D Locational Marginal Pricing

Vaskar Sarkar and S. A. Khaparde, *Senior Member, IEEE*

***Abstract*—The objective of this paper is to suggest a robust optimal power flow (OPF) framework to perform locational marginal pricing under the scarcity of reactive power. The classical OPF models employed for market clearing either assume infinite reactive power support or make a fully independent representation of the reactive power load. In contrast, a potentially more accurate power flow model is adopted in this paper recognizing the dependence of the level of reactive power consumption on the level of active power consumption. The relationship is primarily modeled by employing the concept of power factor. In addition, there can be load requests with different power factors from the same location. The corresponding locational marginal prices (LMPs) are found to vary not only spatially but also according to power factors. Thus, a two-dimensional LMP variation is finally obtained. A consistent definition of financial transmission rights is also provided and the associated LMP decomposition scheme is described. The model proposed is studied on the IEEE 30-bus system and its distinctive features are noted down and discussed.**

***Index Terms*—Financial transmission right, LMP decomposition, locational marginal price, power factor, reactive power compensation.**

NOMENCLATURE

$\boldsymbol{\delta}$	$(n \times 1)$ vector containing bus voltage angle variables.
η	Total number of bids and offers.
$\theta_{j,k}$	Angle of $Y_{j,k}$.
$\boldsymbol{\lambda^{(k)}}$	$(n \times 1)$ nodal LMP vector corresponding to the kth power factor.
$\boldsymbol{\lambda_c^{(k)}}$	Congestion component of $\boldsymbol{\lambda^{(k)}}$.
$\boldsymbol{\lambda_e^{(k)}}$	Energy component of $\boldsymbol{\lambda^{(k)}}$.
$\boldsymbol{\lambda_{loss}^{(k)}}$	Loss component of $\boldsymbol{\lambda^{(k)}}$.
$\boldsymbol{\Omega}$	$(n \times 1)$ slack weight vector.
$\boldsymbol{f_I}(.)$	$(L \times 1)$ function vector defining line currents for a particular system state.
$f_{loss}(.)$	Function defining aggregated active power loss in the network for a particular system state.
$\boldsymbol{f_Q}(.)$	$(n \times 1)$ function vector defining required reactive power compensations at different buses for a particular system state and load profile.
$\boldsymbol{f_{inj}^p}(.)$	$(n \times 1)$ function vector defining active power flows into the network at different buses for a particular system state.
$\boldsymbol{f_{inj}^q}(.)$	$(n \times 1)$ function vector defining reactive power flows into the network at different buses for a particular system state.
$fr(l)$	"From" end bus of the lth line.
$\boldsymbol{I}$	$(L \times 1)$ vector containing the line current variables.
$\boldsymbol{I_{\max}}$	$(L \times 1)$ line current limit vector.
L	Total number of lines in the system.
m	Total number of the possible power factors.
n	Total number of buses in the system.
$\mathbf{O}_{s,w}$	$(s \times w)$ matrix of all zeros.
$\boldsymbol{P}$	$(\eta \times 1)$ vector containing variables that represent the cleared amounts towards individual bids and offers.
$\boldsymbol{P_{\max}}$	Upper limit on $\boldsymbol{P}$
$\boldsymbol{P_{net,k}^{fix}}$	$(n \times 1)$ parameter vector representing the net nodal inelastic loads corresponding to the kth power factor.
P_{slack}	Variable representing the slack power.
$\boldsymbol{Q}$	$(n \times 1)$ vector (variable) representing the acquired reactive power compensations at different buses.
$\boldsymbol{Q_{\max}}$	$(n \times 1)$ vector representing the upper limits on the reactive power compensation services available at different buses.
$\boldsymbol{Q_{\min}}$	$(n \times 1)$ vector representing the lower limits on the reactive power compensation services available at different buses.
r_l	Resistance of the lth line (in per unit).
$to(l)$	"To" end bus of the lth line.
$\boldsymbol{T_f}$	$(m \times 1)$ vector containing tangent factors corresponding to the different power factors.
$\boldsymbol{U_s}$	$(s \times s)$ identity matrix.
$W(.)$	Social-welfare function.
$W^{opt}(*)$	Optimal social-welfare as the function of $*$.

Manuscript received December 22, 2011; revised March 14, 2012 and April 25, 2012; accepted May 26, 2012. Date of publication July 19, 2012; date of current version January 17, 2013. Paper no. TPWRS-01228-2011.

V. Sarkar is with the Department of Electrical Engineering, Indian Institute of Technology Hyderabad, Yeddumailaram 502205, India (e-mail: vaskar@iith.ac.in).

S. A. Khaparde is with the Department of Electrical Engineering, Indian Institute of Technology Bombay, Mumbai 400076, India (e-mail: sak@ee.iitb.ac.in).

Digital Object Identifier 10.1109/TPWRS.2012.2202696

x_l	Reactance of the lth line (in per unit).
$\boldsymbol{Y}$	$(n \times n)$ bus admittance matrix (in per unit).
$\mathbf{0}_{\boldsymbol{s}}$	$(s \times 1)$ vector of all zeros.
$\mathbf{1}_{\boldsymbol{s}}$	$(s \times 1)$ vector of all ones.
$(.)^*$	Optimal solution of a primal variable or KKT solution of a dual variable.
$(.)'$	Column vector containing all the elements of the parent vector $(.)$ except for its last element.

I. Introduction

The paradigm shift of the power industry towards open access has raised the critical concern of appropriate energy pricing for generating and load entities. One efficient form of pricing has been evolved through location-based marginal cost calculation based upon prevailing levels of power loss and network congestion. The prices thus come out are called locational marginal prices (LMPs). The principle of locational marginal pricing is essentially based upon the theory of spot pricing proposed by Schweppe *et al.* [1]. The practice of locational marginal pricing is gradually finding its way to become a global choice through its strong implication of optimal energy pricing and efficient price signaling for new expansions.

There is a wide range of optimal power flow (OPF) models suggested in literature to find locational marginal prices. The models can be broadly classified into two categories, namely, the DC optimal power flow (DCOPF) model [2]–[5] and the AC optimal power flow (ACOPF) model [6]–[12]. The DCOPF model is usually more preferred compared to the ACOPF model because of its inherent simplicity, robustness and capability of fast convergence. However, the applicability of the DCOPF model is limited only to the systems for which the reactive power compensation is never exhausted. This is because the DCOPF model is effectively an "active power only" model having no consideration for the reactive power usage of the system. Thus, although mathematically robust in solution performance, the DCOPF model may practically fail to produce a credible power flow result when the scope of reactive power compensation is inadequate.

Similarly to the DCOPF models, the ACOPF models suggested in [6] and [7] are also based upon the assumption of unlimited reactive power supply, and, therefore, have a limited scope of application. The significance of reactive power in the network operation is explicitly recognized in [8]–[12] by writing down the necessary constraint forms. The OPF models proposed in [8]–[11] are, in effect, based upon the assumption that the loads are purely inelastic. Therefore, the reactive power demand is equivalently considered as an independent constant quantity while performing the generation and load scheduling. Such an independent representation of reactive power load is, however, inappropriate in the case the loads are price sensitive. In general, the reactive power requirement of a load entity varies depending upon the level of its active power consumption. It is, therefore, essential to represent the reactive power demand in suitable function form in the case the active power load is made variable in the OPF formulation.

The connection between the nodal active and reactive power demands is recognized in [12] by employing a linear relationship between the aggregated quantities. The particular functional relationship is modeled by assigning a load power factor for each bus. Such a gross linear representation, however, also does not seem to be very accurate. One obvious reason for this is that there can be multiple types of loads at a bus, each with a different power factor. The further complication may arise in the case there are more than one load (or load serving) entities at the same bus. This is because the mutual consensus between the load entities is then required to decide the load power factor of the respective bus. At the same time, the pricing rule suggested in [12] may not be appropriate for the generating entities.

In this paper, an enhanced framework is developed to make a more accurate representation of reactive power load in the LMP calculation. The enhancement is sought by considering the possibility of a load classification according to the nature of reactive power absorption. Thus, instead of considering a single power factor for all the loads, provision is created to assign different power factors to different loads at any location. The single variable model (for the reactive power load representation) of [12] is thus converted into a multi-variable model rendering more flexibility to enhance the power flow accuracy. It is to be noted that the power factor assigned to a load element should cover both its own reactive power consumption as well as its contribution into the reactive power loss in the corresponding distribution network. The exercises of identifying the contributions of a load element into the distribution system real and reactive power losses could be similar. A two-dimensional definition of locational marginal prices is accordingly provided maintaining consistency with such load classification. Here, the dimensions are specified in terms of the location and the power factor. The different concepts of location, such as node, load zone, and hub [13]–[16], are carefully addressed. A consistent representation of generators is also made to fit the above two-dimensional energy pricing. The modified definition of financial transmission rights (FTRs) [17], [18] with this new pricing rule is subsequently established, and their implementation concerns are discussed in fine details. It is, however, important to understand that the objective of this paper is not to overrule the merits of the existing OPF frameworks. The OPF model suggested in this paper is rather designed specifically for a reactive power constrained scenario with price-sensitive loads for which the existing OPF models may not be appropriate.

The rest of the paper is organized as follows: The required bid format for the new market model is discussed in Section II. The mathematical formulation of the corresponding optimal power flow problem is shown in Section III along with the derivation of locational marginal prices. In Section IV, the issues related to financial transmission rights are resolved. The framework proposed is explained with a numerical example in Section V. The case study performed to illustrate the distinct characteristics of the proposed model is presented in Section VI. Finally, the paper is concluded in Section VII.

II. Bid Format for the Proposed Market Model

The framework proposed provides the flexibility to a load serving entity to submit separate bids for different power factors. Each load bid should then have four components, namely, a MW request, a price quotation, the locational information and a power factor specification. The self-scheduled requests are also to be submitted in the same way, but without quoting any price. The pricing framework proposed also supports the concept of load zone that is in practice in several electricity markets. It is eventually possible to separately specify the load power factor for each of the constituent buses of a load zone instead of specifying a single power factor for the entire load zone.

The representation of a generation offer in the proposed pricing framework requires distinct attention. A physical generator plays the dual role both as an active power source and as a reactive power source. The reactive power capability [19] of a generator can be compactly represented as follows:

$$f_{lo}(P_G, V_G) \leq Q_G \leq f_{up}(P_G, V_G) \tag{1}$$

where P_G and Q_G are the active and reactive power output levels of the generator, and V_G indicates the generator terminal voltage. The functions $f_{up}(.)$ and $f_{lo}(.)$ are monotonically decreasing and increasing, respectively, with P_G. It is obvious that the capability of a generator to produce reactive power varies depending upon the level of its active power production. In fact, the reactive power production capability of a generator increases with the decrease in its active power output. Thus, the reactive power production capability of a generator is the lowest when it generates the maximum active power. However, in order to provide a simplified explanation of the concept of LMP dimensions, it is attempted here to avoid the active power dependent forms of the reactive power limits of a generator. Therefore, the use of reactive power from a generator is limited only within the range that is permissible for all its possible active power output levels. The particular range can be defined as follows:

$$f_{lo}(P_{G,\max}, V_G) \leq Q_G \leq f_{up}(P_{G,\max}, V_G). \tag{2}$$

Here, $P_{G,\max}$ indicates the MW capacity of the particular generator. The reactive power capability of the generator that is left as residual is defined in the following:

$$f_{res,incr}(P_G, V_G) = f_{up}(P_G, V_G) - f_{up}(P_{G,\max}, V_G) \tag{3}$$
$$f_{res,decr}(P_G, V_G) = f_{lo}(P_{G,\max}, V_G) - f_{lo}(P_G, V_G). \tag{4}$$

The function $f_{res,incr}(.)$ basically indicates the upper limit for the further increase of the reactive power output of the generator beyond the range defined in (2). Similarly, $f_{res,decr}(.)$ indicates the upper limit for the further decrease of the reactive power output of the generator beyond the range of (2). The primary difficulty that is observed to use the above residual capacity is in defining a convenient form of pricing for the generators. The problem may be resolved through a linearized representation of the residual reactive power capability of a generator. At the same time, the residual portion of the reactive power capability may be procured either on voluntary basis or on mandatory base. For the second case, an opportunity cost [11], [12] must be paid to the respective generator. However, as mentioned previously, the entire exercise is carried out in this paper based upon the conservative form shown in (2). The unused portion of the reactive power capability of a generator, because of the simplification in (2), may also not be significant in the case $P_{G,\max}$ is well away from the right hand boundary of the capability curve.

The form shown in (2) makes it possible to represent the active and reactive power outputs of a generator as independent control variables. With the particular simplified representation of the reactive power limits of a generator, the generator can now be virtually split into a purely active power source and a purely reactive power source. The power supplied by the corresponding active power source does not have any reactive component, and, thus, can equivalently be assigned a unity power factor. The generation offers can be seen to be received only from these active power sources. A generation offer is then complete with only MW, location and price specifications. The reactive power support of the generator can subsequently be visualized in the form of an independent reactive power compensator. The entire procedure remains the same while dealing with aggregated pricing nodes such as trading hubs.

The format of an "up to congestion charge" bid (that is submitted for executing a bilateral transaction) can be defined in a similar line. The specifications that should be involved in an "up to congestion charge" bid are the source location, the sink location, the sink power factor, the price quotation and the MW request. For a power transfer to a load zone, the sink power factor should be specified in vector form. As for a generation offer, there is no need to specify the source power factor for a transaction request and the same can be assigned a fixed value of unity.

III. OPF Formulation

With the consideration of reactive power, it is essential to employ an ACOPF model to perform dispatch scheduling. Albeit it is complex, the ACOPF application has already been proven to be successful in the CAISO market [20]. The CAISO operator employs a full-fledged security constrained ACOPF model that is subsequently solved through successive linearizations by means of intermediate AC power flow calculations. However, for the sake of simplicity, the OPF problem is formulated here with a fixed bus voltage profile (at one per unit) and the security constraints are ignored. Thus, the state variables are limited only to the bus voltage angles. To formulate the relevant OPF problem, it is first required to convert a power factor into the form of "tangent" factor to get the ratio of reactive and active power consumptions. The conversion should be suitably made taking into account the nature (i.e., leading or lagging) of the specified power factor. Subsequently, the OPF formulation for the day-ahead dispatch problem appears as

$$\text{minimize}\{-W(\boldsymbol{P})\} \tag{5}$$

s.t.

$$h_0 : P_{slack} = 0 \tag{6}$$
$$\boldsymbol{h_1} : \boldsymbol{A_p P} - \boldsymbol{P_{net}^{fix}} \boldsymbol{1_m} + \boldsymbol{\Omega} P_{slack} - \boldsymbol{f_{inj}^p}(\boldsymbol{\delta}) = \boldsymbol{0_n} \tag{7}$$
$$\boldsymbol{g_1} : \boldsymbol{f_Q}(\boldsymbol{\delta}, \boldsymbol{P}, \boldsymbol{P_{net}^{fix}}) - \boldsymbol{Q_{\max}} \leq \boldsymbol{0_n} \tag{8}$$
$$\boldsymbol{g_2} : -\boldsymbol{f_Q}(\boldsymbol{\delta}, \boldsymbol{P}, \boldsymbol{P_{net}^{fix}}) + \boldsymbol{Q_{\min}} \leq \boldsymbol{0_n} \tag{9}$$
$$\boldsymbol{g_3} : \boldsymbol{f_I}(\boldsymbol{\delta}) - \boldsymbol{I_{\max}} \leq \boldsymbol{0_L} \tag{10}$$

$$\boldsymbol{q_1}: \boldsymbol{P} - \boldsymbol{P}_{\max} \leq \boldsymbol{0_\eta} \quad (11)$$
$$\boldsymbol{q_2}: -\boldsymbol{P} \leq \boldsymbol{0_\eta} \quad (12)$$

where

$$\boldsymbol{P_{net}^{fix}} = [\boldsymbol{P_{net,1}^{fix}}\ \boldsymbol{P_{net,2}^{fix}}\ \dots\ \boldsymbol{P_{net,m}^{fix}}] \quad (13)$$

$$\begin{aligned}\boldsymbol{Q} &= \boldsymbol{f_Q}(\boldsymbol{\delta}, \boldsymbol{P}, \boldsymbol{P_{net}^{fix}}) \\ &= \boldsymbol{f_{inj}^q}(\boldsymbol{\delta}) - \boldsymbol{A_q}\boldsymbol{P} + \boldsymbol{P_{net}^{fix}}\boldsymbol{T_f} \end{aligned} \quad (14)$$

$$f_{inj,i}^p(\boldsymbol{\delta}) = Base\_MVA \times \sum_{j=1}^{n} |Y_{i,j}| cos(\theta_{i,j} + \delta_j - \delta_i) \quad (15)$$

$$f_{inj,i}^q(\boldsymbol{\delta}) = -Base\_MVA \times \sum_{j=1}^{n} |Y_{i,j}| sin(\theta_{i,j} + \delta_j - \delta_i) \quad (16)$$

$$I_l = f_{I,l}(\boldsymbol{\delta}) = \sqrt{\frac{2 - 2\cos\left(\delta_{fr(l)} - \delta_{to(l)}\right)}{{r_l}^2 + {x_l}^2}}. \quad (17)$$

Here, all the power quantities are expressed in MW or MVAr. The primary objective behind introducing a slack variable term in the above formulation is just to define the LMP decomposition. However, since the slack power is a virtual quantity in the market, the same is forced to become zero through (6). Constraints (7) are the nodal active power balance constraints. The $\boldsymbol{P}$ vector is converted into the form of nodal active power injections by means of the $n \times \eta$ conversion matrix $\boldsymbol{A_p}$. For example, in the case there is no hub or load zone, the $\boldsymbol{A_p}$ matrix can simply be derived as follows:

$$\begin{aligned} A_{p,i,j} &= 1 \quad \text{if } P_j \text{ is a generation at Bus } i \\ &= -1 \quad \text{if } P_j \text{ is a load at Bus } i \\ &= 0 \quad \text{if } P_j \text{ is not related to Bus } i. \end{aligned} \quad (18)$$

In the same way, the matrix $\boldsymbol{A_q}$ (that is also $n \times \eta$) shown in (14) derives the reactive power injection pattern corresponding to $\boldsymbol{P}$. The particular matrix can be obtained as follows:

$$\begin{aligned} A_{q,i,j} &= -T_{f,k} \quad \text{if} P_j \text{ is a load of } k\text{th power factor at Bus } i \\ &= 0 \quad \text{if } P_j \text{ is not a load at Bus } i. \end{aligned} \quad (19)$$

For any participation from a load zone or hub, the entries of the corresponding column of $\boldsymbol{A_p}$ or $\boldsymbol{A_q}$ should be set according to the specified distribution vector. It should be noted that the entries of $\boldsymbol{A_q}$ corresponding to the generation offers are always zero. This is because a generation offer is seen to be received from a purely active power source and the reactive power produced by the respective generator is treated as an independent shunt compensation. Among the other constraints, the reactive power compensation limits are defined in (8) and (9). Constraints (10) are the line capacity constraints. Here, the line capacities are specified in terms of line current limits. Alternatively, the active power flow (lossless) over a line can also be defined as the limiting quantity for the capacity of the line. Finally, constraints (11) and (12) define the upper and lower limits on the bid and offer variables.

The Lagrangian function of the optimization problem (5)–(12) can be written as

$$\begin{aligned}\Lambda = -W(\boldsymbol{P}) + \nu_0 h_0 + \boldsymbol{\nu_1}^T \boldsymbol{h_1} + \boldsymbol{\mu_1}^T \boldsymbol{g_1} + \boldsymbol{\mu_2}^T \boldsymbol{g_2} \\ + \boldsymbol{\mu_3}^T \boldsymbol{g_3} + \boldsymbol{\vartheta_1}^T \boldsymbol{q_1} + \boldsymbol{\vartheta_2}^T \boldsymbol{q_2}. \end{aligned} \quad (20)$$

Therefore, the nodal LMP vector $\boldsymbol{\lambda^{(k)}}$ corresponding to the kth power factor can be derived as follows:

$$\begin{aligned}\boldsymbol{\lambda^{(k)}} &= -\left\{ \frac{\partial W^{opt}(\boldsymbol{P_{net}^{fix}})}{\partial \boldsymbol{P_{net,k}^{fix}}} \right\}^T \\ &= -\boldsymbol{\nu_1^*} + T_{f,k}\boldsymbol{\mu_1^*} - T_{f,k}\boldsymbol{\mu_2^*}. \end{aligned} \quad (21)$$

Here, $\boldsymbol{\nu_1^*}$, $\boldsymbol{\mu_1^*}$, and $\boldsymbol{\mu_2^*}$ indicate the KKT solutions (that are obtained by solving the KKT necessary conditions of optimality) of the respective dual variables. The formula derived in (21) is based upon the theory of sensitivity analysis [21], which is applicable both for convex and non-convex optimization problems as well as both for locally and globally optimal solutions. The LMP for a load zone corresponding to a specific nodal power factor combination can be obtained simply by taking the weighted sum of respective nodal prices according to the specified load zone distribution vector. The hub LMPs are also obtained in the same way. The price to be paid by a load is equal to the LMP at its location corresponding to its specified power factor. Generators are essentially paid according to LMPs corresponding to the unity power factor. Finally, the network usage price for a bilateral transaction can be obtained by taking the LMP difference between its sink and source locations at the appropriate power factors.

It is obvious that if there is adequate reactive power support at Bus i, both $\mu_{1,i}^*$ and $\mu_{2,i}^*$ will be zero. Therefore, according to (21), there will be a unique LMP at Bus i irrespective of the power factor. On the other hand, if there is a shortage of inductive reactive power at Bus i, constraint (8) will be active at the particular bus. Thus, $\mu_{1,i}^*$ will now be a positive number rendering a higher value of LMP for a higher value of the tangent factor. The LMP for a lagging power factor will then be higher than the LMP for a leading power factor. The reverse phenomenon will happen if there is a shortage of capacitive reactive power at Bus i. It is to be noted that both $\mu_{1,i}^*$ and $\mu_{2,i}^*$ are non-negative numbers. However, both of them cannot be non-zero at the same time.

The expression of the nodal LMP vector corresponding to the kth power factor can be put down in a compact form as follows:

$$\begin{aligned}\boldsymbol{\lambda^{(k)}} &= -\boldsymbol{\nu_1^*} + T_{f,k}\boldsymbol{\mu_1^*} - T_{f,k}\boldsymbol{\mu_2^*} \\ &= -\boldsymbol{\nu_1^*} \\ &\quad + T_{f,k}\{\boldsymbol{U_n}\boldsymbol{\mu_1^*} - \boldsymbol{U_n}\boldsymbol{\mu_2^*} + \mathbf{O}_{\boldsymbol{n},\boldsymbol{L}}\boldsymbol{\mu_3^*}\} \\ &= -\boldsymbol{\nu_1^*} + T_{f,k}\boldsymbol{\Theta}^T\boldsymbol{\mu^*} \end{aligned} \quad (22)$$

where

$$\boldsymbol{\mu}^* = [\boldsymbol{\mu_1^{*T}}\ \boldsymbol{\mu_2^{*T}}\ \boldsymbol{\mu_3^{*T}}]^T \quad (23)$$
$$\boldsymbol{\Theta} = [\boldsymbol{U_n}\ \ -\boldsymbol{U_n}\ \mathbf{O}_{\boldsymbol{n},\boldsymbol{L}}]^T. \quad (24)$$

In the case of unity power factor, $T_{f,k}$ is zero. Therefore

$$\boldsymbol{\lambda}^{(\boldsymbol{upf})} = -\boldsymbol{\nu}_{\mathbf{1}}^{*}. \tag{25}$$

Similarly, in the case of unity tangent factor (corresponding to the lagging power factor of 0.7071), $T_{f,k}$ is one. Therefore

$$\boldsymbol{\lambda}^{(\boldsymbol{utf})} = -\boldsymbol{\nu}_{\mathbf{1}}^{*} + \boldsymbol{\Theta}^{T}\boldsymbol{\mu}^{*}. \tag{26}$$

Here, $\boldsymbol{\lambda}^{(\boldsymbol{upf})}$ and $\boldsymbol{\lambda}^{(\boldsymbol{utf})}$ are the nodal LMP vectors corresponding to unity power factor and unity tangent factor, respectively. From (25) and (26)

$$\boldsymbol{\Theta}^{T}\boldsymbol{\mu}^{*} = \boldsymbol{\lambda}^{(\boldsymbol{utf})} - \boldsymbol{\lambda}^{(\boldsymbol{upf})}. \tag{27}$$

After replacing (25) and (27) into (22), the following relationship is obtained:

$$\boldsymbol{\lambda}^{(\boldsymbol{k})} = \boldsymbol{\lambda}^{(\boldsymbol{upf})} + T_{f,k}(\boldsymbol{\lambda}^{(\boldsymbol{utf})} - \boldsymbol{\lambda}^{(\boldsymbol{upf})}). \tag{28}$$

It is, therefore, sufficient to post the LMPs only for the power factors of 1 and 0.7071 (lagging). The LMPs for other power factors can be derived directly by employing (28). The formula shown in (28) is specifically useful to generate clear price signals for the future investments.

It is to be noted that the price separation occurring at a bus is a natural consequence of recognizing the interdependence of active and reactive power loads in a reactive power constrained dispatch scheduling. This is a similar paradigm shift as did take place during the evolution of locational marginal pricing from the original practice of system-wide uniform pricing. Such price separation is required basically to preserve the essential properties of marginal pricing (see the Case Study section) if more of the system features is to be integrated in the market clearing.

The decomposition of the nodal LMP vector can be performed by following the same procedure as is shown in [6]. According to the KKT necessary conditions of optimality

$$\frac{\partial\Lambda}{\partial\boldsymbol{\delta}'} = -\boldsymbol{\nu}_{\mathbf{1}}^{*T}\frac{\partial \boldsymbol{f}_{\boldsymbol{inj}}^{\boldsymbol{p}}}{\partial\boldsymbol{\delta}'}(\boldsymbol{\delta}^{*}) + \boldsymbol{\mu}^{*T}\frac{\partial \boldsymbol{f}_{\boldsymbol{cap}}}{\partial\boldsymbol{\delta}'}(\boldsymbol{\delta}^{*}) = \mathbf{0}_{\boldsymbol{n-1}}^{T} \tag{29}$$

$$\frac{\partial\Lambda}{\partial P_{slack}} = \boldsymbol{\nu}_{\mathbf{1}}^{*T}\boldsymbol{\Omega} + \nu_0^{*} = 0 \tag{30}$$

where

$$\boldsymbol{f}_{\boldsymbol{cap}}(\boldsymbol{\delta}) = [\boldsymbol{f}_{\boldsymbol{inj}}^{\boldsymbol{q}}(\boldsymbol{\delta})^{T} \quad -\boldsymbol{f}_{\boldsymbol{inj}}^{\boldsymbol{q}}(\boldsymbol{\delta})^{T} \quad \boldsymbol{f}_{\boldsymbol{I}}(\boldsymbol{\delta})^{T}]^{T} \tag{31}$$

$$\boldsymbol{\delta}' = [\delta_1\ \delta_2\ \ldots\delta_{n-1}]^{T}. \tag{32}$$

Here, the nth bus is taken as the angle reference bus. The relationships shown in (29) and (30) can be compactly written as follows:

$$\boldsymbol{\nu}_{\mathbf{1}}^{*T}\underbrace{\begin{bmatrix}\dfrac{\partial \boldsymbol{f}_{\boldsymbol{inj}}^{\boldsymbol{p}}}{\partial\boldsymbol{\delta}'}(\boldsymbol{\delta}^{*}) & -\boldsymbol{\Omega}\end{bmatrix}}_{\hat{\boldsymbol{J}}} = \begin{bmatrix}\boldsymbol{\mu}^{*T}\dfrac{\partial \boldsymbol{f}_{\boldsymbol{cap}}}{\partial\boldsymbol{\delta}'}(\boldsymbol{\delta}^{*}) & \nu_0^{*}\end{bmatrix}. \tag{33}$$

Therefore

$$\boldsymbol{\nu}_{\mathbf{1}}^{*T}\hat{\boldsymbol{J}} = \boldsymbol{\mu}^{*T}\begin{bmatrix}\dfrac{\partial \boldsymbol{f}_{\boldsymbol{cap}}}{\partial\boldsymbol{\delta}'}(\boldsymbol{\delta}^{*}) & \mathbf{0}_{\boldsymbol{2n+L}}\end{bmatrix} + \nu_0^{*}\begin{bmatrix}\mathbf{0}_{\boldsymbol{n}-1}^{T} & 1\end{bmatrix}. \tag{34}$$

The second term on the right hand side of (34) can be decomposed as follows:

$$\begin{bmatrix}\mathbf{0}_{\boldsymbol{n-1}}^{T} & 1\end{bmatrix} = -1_{\boldsymbol{n}}^{T}\hat{\boldsymbol{J}} + \begin{bmatrix}\dfrac{\partial\{1_{\boldsymbol{n}}^{T}\boldsymbol{f}_{\boldsymbol{inj}}^{\boldsymbol{p}}\}}{\partial\boldsymbol{\delta}'}(\boldsymbol{\delta}^{*}) & 0\end{bmatrix}. \tag{35}$$

It should be noted that $1_{\boldsymbol{n}}^{T}\boldsymbol{\Omega} = 1$. Let the matrix $\boldsymbol{S}$ and the vector $\boldsymbol{L}_{\boldsymbol{F}}$ be defined as follows:

$$\boldsymbol{S} = \begin{bmatrix}\dfrac{\partial \boldsymbol{f}_{\boldsymbol{cap}}}{\partial\boldsymbol{\delta}'}(\boldsymbol{\delta}^{*}) & \mathbf{0}_{\boldsymbol{2n+L}}\end{bmatrix}\hat{\boldsymbol{J}}^{-1} \tag{36}$$

$$\boldsymbol{L}_{\boldsymbol{F}}^{T} = \begin{bmatrix}\dfrac{\partial\{1_{\boldsymbol{n}}^{T}\boldsymbol{f}_{\boldsymbol{inj}}^{\boldsymbol{p}}\}}{\partial\boldsymbol{\delta}'}(\boldsymbol{\delta}^{*}) & 0\end{bmatrix}\hat{\boldsymbol{J}}^{-1}. \tag{37}$$

Therefore, after replacing (35) into (34), $\boldsymbol{\nu}_{\mathbf{1}}^{*}$ can be expressed in the following form:

$$\boldsymbol{\nu}_{\mathbf{1}}^{*} = -\nu_0^{*}1_{\boldsymbol{n}} + \nu_0^{*}\boldsymbol{L}_{\boldsymbol{F}} + \boldsymbol{S}^{T}\boldsymbol{\mu}^{*}. \tag{38}$$

Subsequently, (38) can be replaced in (22) to yield the following alternative expression for the nodal LMP vector:

$$\boldsymbol{\lambda}^{(\boldsymbol{k})} = \nu_0^{*}\mathbf{1}_{\boldsymbol{n}} - \nu_0^{*}\boldsymbol{L}_{\boldsymbol{F}} - \underbrace{\{\boldsymbol{S} - T_{f,k}\boldsymbol{\Theta}\}}_{\hat{\boldsymbol{S}}^{(\boldsymbol{k})}}{}^{T}\boldsymbol{\mu}^{*}. \tag{39}$$

It is obvious that

$$f_{loss}(\boldsymbol{\delta}) = 1_{\boldsymbol{n}}^{T}\boldsymbol{f}_{\boldsymbol{inj}}^{\boldsymbol{p}}(\boldsymbol{\delta}). \tag{40}$$

Therefore, the elements of the $\boldsymbol{L}_{\boldsymbol{F}}$ vector are essentially the sensitivity factors relating the active power loss in the network to the specified nodal active power injections. In the same way, the matrix $\hat{\boldsymbol{S}}^{(\boldsymbol{k})}$ defines the sensitivities of the capacity-constrained system quantities (i.e., $\boldsymbol{Q}$, $-\boldsymbol{Q}$, and $\boldsymbol{I}$) to the specified nodal active power injections corresponding to the kth power factor. It is obvious that $\hat{\boldsymbol{S}}^{(\boldsymbol{upf})} = \boldsymbol{S}$, where $\hat{\boldsymbol{S}}^{(\boldsymbol{upf})}$ is the constraint sensitivity matrix with respect to active power injections at unity power factor. Therefore

$$\hat{\boldsymbol{S}}^{(\boldsymbol{k})} = \hat{\boldsymbol{S}}^{(\boldsymbol{upf})} - T_{f,k}\boldsymbol{\Theta}. \tag{41}$$

It should be noted that, unlike the constraint sensitivity factors, the loss sensitivity factors are unique for all the power factors.

According to (39), the nodal LMP vector corresponding to the kth power factor can be decomposed into energy, loss and congestion components as follows:

$$\boldsymbol{\lambda}_{\boldsymbol{e}}^{(\boldsymbol{k})} = \nu_0^{*}1_{\boldsymbol{n}},\ \boldsymbol{\lambda}_{\boldsymbol{loss}}^{(\boldsymbol{k})} = -\nu_0^{*}\boldsymbol{L}_{\boldsymbol{F}},\ \boldsymbol{\lambda}_{\boldsymbol{c}}^{(\boldsymbol{k})} = -\hat{\boldsymbol{S}}^{(k)^{T}}\boldsymbol{\mu}^{*}. \tag{42}$$

It is obvious that

$$\begin{aligned}\boldsymbol{\lambda}_{\boldsymbol{c}}^{(\boldsymbol{k})} &= \boldsymbol{\lambda}_{\boldsymbol{c}}^{(\boldsymbol{upf})} + T_{f,k}\boldsymbol{\Theta}^{T}\boldsymbol{\mu}^{*}\\ &= \boldsymbol{\lambda}_{\boldsymbol{c}}^{(\boldsymbol{upf})} + T_{f,k}(\boldsymbol{\lambda}^{(\boldsymbol{utf})} - \boldsymbol{\lambda}^{(\boldsymbol{upf})}).\end{aligned} \tag{43}$$

The LMP components for a load zone (or hub) can be obtained simply be aggregating the corresponding LMP components at the constituent nodes.

The OPF formulation shown above is still based upon the consideration of a market for only active power. The LMP framework proposed is also suitable for a combined active and reactive power market as was suggested in [10]–[12]. A separate set of LMPs can, therefore, be established for the reactive power compensations by inviting price offers from the respective market players. The reactive power payment of a load entity will, however, be embedded in its payment for the active power. This is because the reactive power request of the load entity is in itself embedded in its active power request through a power factor specification. Therefore, even in the presence of a reactive power market, the LMPs for the active power must be defined over two dimensions in the case the interdependence of active and reactive power loads is to be recognized.

The consideration of a fixed bus voltage profile is not a hard requirement to implement the proposed framework. The market optimization model [i.e., (5)–(12)] can easily be modified by incorporating the voltage variables and the associated constraints. This will also not change the LMP expression as is shown in (21). However, the LMP decomposition in the case of a variable bus voltage based formulation is still not well defined. The practical purpose of LMP decomposition is just to make the settlement of FTRs. Therefore, even though there can be separate prices for reactive power, the LMPs that are established for active power are only to be decomposed for any practical application. Typically, the LMP decomposition is performed in such a way that the loss component disappears for zero active power loss and the congestion component disappears for no congestion. At the same time, the congestion component is required to be expressed as a weighted sum of the constraint shadow prices. The weighting factors for the same should be chosen as the constraint sensitivities to the active power withdrawal at the corresponding location. In the case of a fixed bus voltage profile based formulation, those sensitivity terms can be uniquely defined [as in (39)]. However, no such unique definition of constraint sensitivities to nodal active power injections (or withdrawals) exists when the bus voltages are made variable. In [8] and [10], the constraint sensitivities to nodal active power injections are basically defined with respect to fixed nodal reactive power injections. The primary problem associated with such LMP decomposition is that the loss component will not be zero even though the active power loss in the system is zero. Instead of fixing the reactive power injections, the bus voltage magnitudes may, however, be set fixed (at the optimal values obtained by solving the market optimization) in order to perform the LMP decomposition. This will produce a similar result as above satisfying all the basic properties of LMP decomposition. However, there can also be other ways to define constraint sensitivities in order to produce a meaningful LMP decomposition in the case of variable bus voltage consideration.

IV. FTR Implementation

With the new LMP framework in place, the parametric definition of FTRs should also be consistently updated. The modified FTR definition should now include a couple of power factor terms (scalar or vector) in addition to the conventional specifications of source, sink, MW amount and time of validity. Those power factors are to be specified for the source and sink locations, respectively, and will have a direct impact on the hourly evaluation of FTRs. The source power factors of the FTRs can, however, be set fixed at unity. The same is prescribed based upon the consideration that FTRs are basically made for compensating the congestion payments of the bilateral transactions.

Ideally, the evaluation of an FTR should be carried out based upon the LMP difference between its sink and source locations (at the specified power factors). However, because of the revenue adequacy issue, only the congestion components of locational prices can practically be considered for the FTR evaluation. This in turn makes the FTR values reference dependent. Therefore, a suitable criterion must be established for the selection of the slack weight vector to perform LMP decomposition. In this regard, an optimization-based methodology was proposed in [22] to decompose traditional (i.e., one-dimensional) locational marginal prices. The same methodology can also be adopted for the 2-D LMP decomposition. From (42), the congestion components of locational marginal prices (nodal) at unity power factor can be written down as follows:

$$\boldsymbol{\lambda_c^{(upf)}} = -\hat{\boldsymbol{S}}^{(upf)^T}\boldsymbol{\mu}^*. \tag{44}$$

By following the same procedure as in [22], $\boldsymbol{\lambda_c^{(upf)}}$ can subsequently be expressed in the following form:

$$\boldsymbol{\lambda_c^{(upf)}} = \boldsymbol{v^{(upf)}}\lambda_{c,n}^{(upf)} + \boldsymbol{u^{(upf)}} \tag{45}$$

where

$$\boldsymbol{v^{(upf)}} = \begin{bmatrix} -\{\boldsymbol{J_{11}^T}\}^{-1}\boldsymbol{J_{21}^T} \\ 1 \end{bmatrix} \tag{46}$$

$$\boldsymbol{u^{(upf)}} = \begin{bmatrix} \{\boldsymbol{J_{11}^T}\}^{-1}\boldsymbol{K} \\ 0 \end{bmatrix} \tag{47}$$

$$\boldsymbol{K} = -\left\{\frac{\partial \boldsymbol{f_{cap}}}{\partial \boldsymbol{\delta}'}(\boldsymbol{\delta}^*)\right\}^T \boldsymbol{\mu}^* \tag{48}$$

$$\hat{\boldsymbol{J}} = \begin{bmatrix} \boldsymbol{J_{11}} & \boldsymbol{J_{12}} \\ \boldsymbol{J_{21}} & \boldsymbol{J_{22}} \end{bmatrix}. \tag{49}$$

Here, $\boldsymbol{J_{11}}$ is $(n-1)\times(n-1)$ and $\boldsymbol{J_{21}}$ is $1\times(n-1)$. The elements $\boldsymbol{J_{12}}$ and $\boldsymbol{J_{22}}$ are simply $\{-\boldsymbol{\Omega}'\}$ and $\{-\Omega_n\}$, respectively. For any specific instance of the given OPF formulation, both $\boldsymbol{v^{(upf)}}$ and $\boldsymbol{u^{(upf)}}$ are constants and do not depend upon $\boldsymbol{\Omega}$. The following relationship can further be established to determine $\boldsymbol{\Omega}$ for a given value of $\lambda_{c,n}^{(upf)}$:

$$\lambda_{c,n}^{(upf)} = \frac{\boldsymbol{\Omega}'^T\boldsymbol{u^{(upf)}}'}{\boldsymbol{\Omega}'^T(\boldsymbol{1_{n-1}} - \boldsymbol{v^{(upf)}}') - 1}. \tag{50}$$

The explanation of the symbol $(.)'$ is provided in the Nomenclature section.

From (43) and (45), the congestion component of the nodal LMP vector corresponding to the kth power factor can be expressed as

$$\begin{aligned}\boldsymbol{\lambda_c^{(k)}} &= \boldsymbol{v^{(upf)}}\lambda_{c,n}^{(upf)} + \boldsymbol{u^{(upf)}} + T_{f,k}\boldsymbol{\Theta}^T\boldsymbol{\mu}^* \\ &= \boldsymbol{v^{(k)}}\lambda_{c,n}^{(upf)} + \boldsymbol{u^{(k)}}.\end{aligned} \tag{51}$$

Here, $\boldsymbol{v^{(k)}}$ is the same as $\boldsymbol{v^{(upf)}}$ and $\boldsymbol{u^{(k)}}$ is obtained by adding $T_{f,k}\boldsymbol{\Theta}^T\boldsymbol{\mu}^*$ to $\boldsymbol{u^{(upf)}}$. Similarly to $\boldsymbol{u^{(upf)}}$, $\boldsymbol{u^{(k)}}$ is also slack independent since $\boldsymbol{\mu}^*$, in itself, is independent of $\boldsymbol{\Omega}$. Consequently, all the FTR values can now be expressed as linear functions of $\lambda_{c,n}^{(upf)}$. The optimal LMP decomposition task can subsequently be formulated in the form of a simple quadratic programming problem with only one variable (that is, $\lambda_{c,n}^{(upf)}$) and two constraints. The optimal solution for $\lambda_{c,n}^{(upf)}$ thus obtained can then be substituted in (50) and (51) to get the optimal solution for the slack weight vector and the other congestion prices.

As was discussed in [22], the classical concept of revenue adequacy test for FTRs may not be suitable in the case of ACOPF-based LMP evaluation. The simultaneous feasibility criterion for the issuance of FTRs is still meaningful from the point of view of a successful execution of the associated bilateral power transactions. At the same time, the congestion component of an LMP differential can also be ensured to be closely equal to the total LMP differential by enforcing the simultaneous feasibility condition. The simultaneous feasibility test of FTRs can satisfactorily be performed by using a simple DC power flow model in the case there is unlimited reactive power support for the system. However, for a reactive power scarce scenario, as is the consideration made here, the simultaneous feasibility test should be carried out only by using the corresponding AC power flow model and by verifying both reactive power and line flow limits. A good estimation of the future unit commitment pattern is required in this regard so as to appropriately count the reactive power availability at the generator buses. It is essential to ignore active power losses in the network while performing the simultaneous feasibility test. The same is required to maintain consistency with the lossless profile of practically used balanced FTRs.

V. Numerical Example

Consider a four-bus and five-line system. The line information of the particular system is provided in Table I. The base MVA for the system is taken as 100. The reactive power support available at each bus is considered to be within the range of −100 MVAr to 100 MVAr. There is a load zone in the system comprising of Buses 2 and 3 with 3:1 load distribution. Table II shows the generation offers, load bids and transaction bids that are submitted in a certain day-ahead market. There is also a price-insensitive load request of 20 MW from Bus 2 at unity power factor. In addition, there is a self-scheduled ("self-scheduled" and "price-insensitive" are synonymous) bilateral transaction of 100 MW from Bus 4 to the above load zone. The power factors for the respective transaction are specified to be 0.8 (leading) at Bus 3 and unity at Bus 2. The particular bilateral transaction is supported by an FTR of same MW on the same path. The specified power factors for this FTR are unity at Bus 4, 0.8 (lagging) at Bus 2, and 0.8 (leading) at Bus 3. For the sake of a clear illustration of the result of optimal LMP decomposition, another FTR of 239 MW is arbitrarily assumed from Bus 1 to Bus 3 maintaining simultaneous feasibility. The simultaneous feasibility test is performed with the same capacity limits as are used for the dispatch scheduling. The power factors for the second FTR are taken to be unity both for the source and sink locations.

TABLE I
LINE INFORMATION

Line no.	From	To	Reactance (p.u.)	Resistance (p.u.)	Capacity (p.u.)
1	2	3	0.15	0.01	1.1
2	3	4	0.15	0.02	2
3	4	1	0.1	0.01	1.2
4	4	2	0.2	0.02	1.2
5	1	2	0.1	0.015	1.5

TABLE II
BID INFORMATION

Bid no.	Type	Bus/ Path	MW amount	Bid price ($/MW)	Power factor
G1	Generator	1	150	20	–
G2	Generator	4	50	25	–
D1	Load	3	160	30	0.9 (lagging)
B1	Transaction	1-3	70	5	1

Note that the power factor for a generation request or the source power factor for a transaction request is always held at unity; therefore, those values are not specified explicitly. It is obvious that the power factors that are of concern here are unity, 0.8 (leading), 0.8 (lagging) and 0.9 (lagging), respectively. The tangent factors corresponding to above power (or cosine) factors are calculated and are put down in vector form as shown follows:

$$\boldsymbol{T_f} = [0 \quad -0.75 \quad 0.75 \quad 0.4843]^T. \tag{52}$$

Subsequently, the nodal fixed load vectors can be derived as follows:

$$\boldsymbol{P_{net,1}^{fix}} = [0 \quad 95 \quad 0 \quad -100]^T \tag{53}$$
$$\boldsymbol{P_{net,2}^{fix}} = [0 \quad 0 \quad 25 \quad 0]^T \tag{54}$$
$$\boldsymbol{P_{net,3}^{fix}} = \boldsymbol{P_{net,4}^{fix}} = [0 \quad 0 \quad 0 \quad 0]^T. \tag{55}$$

Note that $\boldsymbol{T_f}$ can easily be augmented with the other possible tangent factors simply be defining the corresponding fixed load profiles as zero vectors.

The other elements of the OPF model are defined as follows:

$$\boldsymbol{P} = [P_{D1} \quad P_{G1} \quad P_{G2} \quad P_{B1}]^T \tag{56}$$
$$\boldsymbol{P_{\max}} = [160 \quad 150 \quad 50 \quad 70]^T \tag{57}$$
$$\boldsymbol{Q_{\max}} = [100 \quad 100 \quad 100 \quad 100]^T \tag{58}$$
$$\boldsymbol{Q_{\min}} = [-100 \quad -100 \quad -100 \quad -100]^T \tag{59}$$
$$\boldsymbol{I_{\max}} = [1.1 \quad 2 \quad 1.2 \quad 1.2 \quad 1.5]^T \tag{60}$$
$$\boldsymbol{A_p} = \begin{bmatrix} 0 & 1 & 0 & 1 \\ 0 & 0 & 0 & 0 \\ -1 & 0 & 0 & -1 \\ 0 & 0 & 1 & 0 \end{bmatrix} \tag{61}$$
$$\boldsymbol{A_q} = \begin{bmatrix} 0 & 0 & 0 & 0 \\ 0 & 0 & 0 & 0 \\ -0.4843 & 0 & 0 & 0 \\ 0 & 0 & 0 & 0 \end{bmatrix}. \tag{62}$$

Finally, the social welfare function can be formulated as

$$W(\boldsymbol{P}) = 30P_{D1} - 20P_{G1} - 25_{G2} + 5P_{B1}. \tag{63}$$

The respective optimal power flow problem is solved by using GAMS software and the locational marginal prices are obtained as follows:

$$\boldsymbol{\lambda} = \begin{bmatrix} 23.3326 & 23.3326 & 23.3326 & 23.3326 \\ 27.5409 & 27.5409 & 27.5409 & 27.5409 \\ 28.3326 & 25.7503 & 30.9148 & 30 \\ 25 & 25 & 25 & 25 \end{bmatrix} \tag{64}$$

where

$$\boldsymbol{\lambda} = [\,\boldsymbol{\lambda}^{(1)} \quad \boldsymbol{\lambda}^{(2)} \quad \boldsymbol{\lambda}^{(3)} \quad \boldsymbol{\lambda}^{(4)}\,]. \tag{65}$$

Each row of the $\boldsymbol{\lambda}$ matrix essentially shows the corresponding nodal LMP values for different power factors at the same time interval. Therefore, Generators G1 and G2 are paid at \$23.3326/MW and \$25/MW, respectively. On the other hand, Load D1 is charged with a price of \$30/MW and Transaction B1 has to pay a price of \$5/MW. The cleared amounts towards these requests are 150 MW, 24.28 MW, 144.85 MW, and 66.09 MW, respectively. Similarly, the fixed (i.e., price-insensitive) load request of 20 MW is charged with a price of \$27.5409/MW. To calculate the network usage price for the fixed transaction request, it is first required to calculate the LMP for the respective load zone corresponding to the specified set of power factors. The same is obtained by taking the weighted sum of $\lambda_2^{(1)}$ and $\lambda_3^{(2)}$ according to the weighting factors of 0.75 and 0.25, respectively. The load zone LMP is thus obtained to be \$27.09/MW. The network usage price for the respective bilateral transaction can subsequently be calculated to be \$2.09/MW.

For the given set of FTRs, the congestion component of the LMP matrix $\boldsymbol{\lambda}$ can be optimally determined as follows:

$$\boldsymbol{\lambda_c} = \begin{bmatrix} 19.72 & 19.72 & 19.72 & 19.72 \\ 23.77 & 23.77 & 23.77 & 23.77 \\ 24.46 & 21.88 & 27.04 & 26.13 \\ 21.33 & 21.33 & 21.33 & 21.33 \end{bmatrix}. \tag{66}$$

The owners of FTR 1 (i.e., of 100 MW) and FTR 2 (i.e., of 239 MW) are then paid at \$1.97/MW and \$4.74/MW, respectively.

VI. Case Study

The proposed 2-D LMP framework is studied in further details through a market simulation on a modified IEEE 30-bus system. For the modified IEEE 30-bus system, the resistance of each line is taken as the one-tenth of its reactance and the shunt susceptances are ignored. The line reactances are, however, maintained at their original values. The current carrying capacity of a line is determined according to the following formula:

$$I_{\max,l} = \min\left\{7.62, \sqrt{\frac{2 - 2\cos\left(\frac{\pi}{6}\right)}{{r_l}^2 + {x_l}^2}}\right\}. \tag{67}$$

The upper limit of reactive power compensation for each bus is taken to be 105 MVAr. The corresponding lower limit is set at -105 MVAr for all the buses except for Bus 8. For Bus 8, the respective limit is set at -60 MVAr. The base MVA for the particular simulation is assumed to be 100.

TABLE III
Generation Offers and Load Bids

Bid no.	Type	Bus	MW amount	Bid price (\$/MW)	Power factor
G1	Generator	1	96	12	–
G2	Generator	2	46	15	–
G3	Generator	8	108	10	–
G4	Generator	23	93	18	–
G5	Generator	27	77	16	–
D1	Load	3	20	22	0.8 (lagging)
D2	Load	8	15	20	0.8 (leading)
D3	Load	13	20	25	0.8 (lagging)
D4	Load	21	15	22.50	0.8 (lagging)
D5	Load	27	10	24	0.8 (lagging)
D6	Load	5	20	20	0.8 (lagging)
D7	Load	7	20	21.50	0.8 (lagging)
D8	Load	12	10	28	0.8 (lagging)
D9	Load	29	30	25	0.8 (lagging)
D10	Load	23	65	30	0.8 (lagging)
D11	Load	14	20	23.50	0.8 (lagging)
D12	Load	15	15	25.50	0.8 (lagging)
D13	Load	20	50	21	0.8 (lagging)
D14	Load	16	60	21	0.8 (lagging)
D15	Load	18	20	20.50	0.8 (lagging)
D16	Load	19	25	26	0.8 (lagging)

Table III shows the bids and offers that are considered for this study. In addition, there is a self-scheduled load of 10 MW at each of the load locations shown in Table III. The power factor associated with each of the self-scheduled loads is 0.9 (lagging) except for the load at Bus 8. The power factor for the load at Bus 8 is taken to be 0.9 (leading). There is also a total of 272 MW self-scheduled generation request, which is distributed over individual generator locations in the same proportion as the total generation offer of 420 MW (see Table III) is distributed. The bilateral transaction requests received for the particular hour are shown in Table IV. All these requests are obtained in self-scheduled form. Each of the bilateral transactions is also supported by an FTR of same MW on the same path. The FTR associated with Transaction SSBT11 is specified with unity power factor both for the source and sink locations. The power factor specifications of other FTRs are the same as those of the corresponding bilateral transactions. To ensure a hard constrained (i.e., hitting some of the simultaneous feasibility constraint limits) FTR issuance, another FTR of 105 MW is arbitrarily considered between Bus 27 and Bus 19. The power factors for the last FTR are taken to be unity and 0.9 (lagging) for the source and sink locations, respectively. The simultaneous feasibility test is again performed with the same capacity limits as are used for the dispatch scheduling.

The LMP outcome of the particular simulation is shown in Fig. 1. The LMP distribution corresponding to power factors 1, 0.8 (lagging), 0.8 (leading), 0.9 (lagging), and 0.9 (leading) are shown through solid, normal dashed, bold dashed, normal circled, and bold circled curves, respectively. It can be seen that the locational marginal prices for different power factors are clearly separated at Buses 8, 12, and 29. This, in turn, indicates reactive power scarcity at those buses. Moreover, the LMP at Bus 8 goes higher when the power factor changes from lagging to leading. This implies a scarcity of capacitive reactive power

TABLE IV
BILATERAL TRANSACTION REQUESTS

Request no.	From bus	To bus	MW amount	Sink power factor
SSBT1	1	3	40	0.8 (lagging)
SSBT2	2	8	45	0.8 (leading)
SSBT3	2	13	40	0.8 (lagging)
SSBT4	2	21	25	0.8 (lagging)
SSBT5	8	21	20	0.8 (lagging)
SSBT6	8	27	50	0.8 (lagging)
SSBT7	8	5	60	0.8 (lagging)
SSBT8	8	7	60	0.8 (lagging)
SSBT9	8	12	40	0.8 (lagging)
SSBT10	23	12	30	0.8 (lagging)
SSBT11	23	29	70	0.8 (lagging)
SSBT12	23	14	50	0.8 (lagging)
SSBT13	27	15	55	0.8 (lagging)
SSBT14	27	20	20	0.8 (lagging)
SSBT15	27	16	30	0.8 (lagging)
SSBT16	27	19	30	0.8 (lagging)

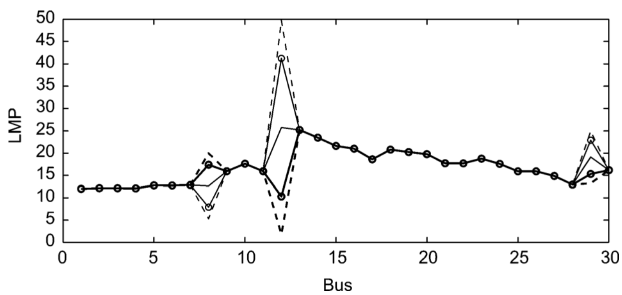

Fig. 1. Spatial LMP distribution.

TABLE V
MARKET CLEARING RESULTS FOR BIDS AND OFFERS

Bid no.	Cleared amount (MW)	Clearing price ($/MW)	Bid no.	Cleared amount (MW)	Clearing price ($/MW)
G1	34.04	12	D7	20	12.88
G2	0	12.16	D8	0	49.74
G3	108	12.65	D9	28.10	25
G4	93	18.77	D10	65	18.77
G5	0	14.88	D11	12.03	23.50
D1	20	12.14	D12	15	21.63
D2	9.35	20	D13	50	19.77
D3	0	25.21	D14	17.63	21
D4	15	17.73	D15	0	20.80
D5	10	14.88	D16	25	20.25
D6	20	12.78	–	–	–

TABLE VI
FINAL POSITIONS OF BILATERAL TRANSACTIONS

Transaction id.	Network usage payment ($/MW)	FTR reimbursement ($/MW)
SSBT1	0.14	0.14
SSBT2	7.84	7.84
SSBT3	13.06	13.06
SSBT4	5.57	5.57
SSBT5	5.08	5.08
SSBT6	2.23	2.23
SSBT7	0.13	0.13
SSBT8	0.23	0.23
SSBT9	37.09	37.09
SSBT10	30.97	30.97
SSBT11	6.23	0.35
SSBT12	4.73	4.73
SSBT13	6.75	6.75
SSBT14	4.89	4.89
SSBT15	6.12	6.12
SSBT16	5.37	5.37

at Bus 8. In the same way, Buses 12 and 29 can be observed to be scarce of inductive reactive power. To prevent the LMP separation, it is, therefore, required to increase the size of the inductor bank at Bus 8 and the sizes of the capacitor banks at Buses 12 and 29. Fig. 1 also illustrates a significant impact of the power factor over locational marginal prices.

Table V presents the summary of the market clearing results that are obtained for load bids and generation offers. It can be easily seen that the price paid to any selected generation offer is no lower than its offer price. Similarly, the price charged to any selected load bid is no higher than its bid price. In the case of any partial selection, the market price for the respective entity is, however, set exactly at the bid or offer price. At the same time, for an unselected generation offer, the concerned entity sees a market price that is lower than its offer price. On the other hand, for an unselected load bid, the concerned entity sees a market price that is higher than its bid price. It can also be verified that a higher offer price than the obtained market price would have resulted in a reduction in the quantity selection. For example, if the offer of Generator G3 would have been made at a price of $13/MW, only 40.84 MW could be selected from this generation offer. A reverse phenomenon happens for the load bids. For example, if Load D12 would have submitted its bid at a price of $21/MW, the bid could not be selected at all. The above facts clearly illustrate a true marginal pricing in the proposed market framework.

The locational marginal prices shown in Fig. 1 are optimally decomposed into energy, loss, and congestion components. The FTR reimbursements are calculated based upon the results of optimal LMP decomposition. The corresponding final positions of bilateral power transaction are shown in Table VI. Here, all the bilateral transactions, except for SSBT11, are able to completely recover the network usage payments through their FTRs. However, the recovered amount is only 5.62% for Transaction SSBT11 although its FTR is defined over the same path and for the same MW. The specific reason behind this anomaly is the power factor mismatch between the bilateral transaction and the corresponding FTR. The particular result clearly illustrates the importance of careful power factor specifications in the procurement of FTRs.

VII. CONCLUSION

The paper introduces a two-dimensional LMP framework to make a more accurate representation of load reactive power in the optimal power flow calculation. The specific application of the model is suggested for a reactive power constrained situation with price-sensitive load requests. The distinctive feature of the proposed model lies in recognizing the interdependence of active and reactive power loads. Thus, the reactive power consumption made by a load entity is modeled as a function of the corresponding active power consumption by employing the concept of power factor. With further precision, a load classification is considered at every location on the basis of a more rigorous power factor estimation. The locational marginal prices are accordingly featured over two dimensions (in terms of location and power factor) preserving all the necessary properties of marginal pricing. The FTR model for the new LMP framework is established and the optimal LMP decomposition is defined. Since the physical loads are usually inductive, the framework developed may also be applicable for a piece-wise linear representation of the relationship between the active and reactive power loads. Such a representation should be necessary in the case a certain quantum of the load reactive power is compensated locally at the distribution substation. The representation of the load reactive power may be further enhanced by introducing more number of dimensions in the LMP definition.

REFERENCES

[1] F. C. Scheweppe, M. C. Caramanis, R. D. Tabors, and R. E. Bohn, *Spot Pricing of Electricity*. Norwell, MA: Kluwer, 1988.

[2] Y. Fu and Z. Li, "Different models and properties on LMP calculations," in *Proc. IEEE/Power Eng. Soc. General Meeting*, Jun. 18–22, 2006.

[3] E. Litvinov, T. Zheng, G. Rosenwald, and P. Shamsollahi, "Marginal loss modeling in LMP calculation," *IEEE Trans. Power Syst*, vol. 19, no. 2, pp. 880–888, May 2004.

[4] F. Li and R. Bo, "DCOPF-based LMP simulation: Algorithm, comparison with ACOPF, and sensitivity," *IEEE Trans. Power Syst*, vol. 22, no. 4, pp. 1475–1485, Nov. 2007.

[5] V. Sarkar and S. A. Khaparde, "DCOPF-based marginal loss pricing with enhanced power flow accuracy by using matrix loss distribution," *IEEE Trans. Power Syst*, vol. 24, no. 3, pp. 1435–1445, Aug. 2009.

[6] T. Wu, Z. Alaywan, and A. D. Papalexopoulos, "Locational marginal price calculations using the distributed-slack power-flow formulation," *IEEE Trans. Power Syst*, vol. 20, no. 2, pp. 1188–1190, May 2005.

[7] T. Orfanogianni and G. Gross, "A general formulation for LMP evaluation," *IEEE Trans. Power Syst*, vol. 22, no. 3, pp. 1163–1173, Aug. 2007.

[8] J. D. Finney, H. A. Othman, and W. L. Rutz, "Evaluating transmission congestion constraints in system planning," *IEEE Trans. Power Syst*, vol. 12, no. 3, pp. 1143–1150, Aug. 1997.

[9] X. Cheng and T. J. Overbye, "An energy reference bus independent LMP decomposition algorithm," *IEEE Trans. Power Syst*, vol. 21, no. 3, pp. 1041–1049, Aug. 2006.

[10] K. Xie, Y. H. Song, J. Stonham, E. Yu, and G. Liu, "Decomposition model and interior point methods for optimal spot pricing of electricity in deregulation environments," *IEEE Trans. Power Syst*, vol. 15, no. 1, pp. 39–50, Feb. 2000.

[11] Y. Dai, Y. X. Ni, C. M. Shen, F. S. Wen, Z. X. Han, and F. F. Wu, "A study of reactive power marginal price in electricity market," *Elect. Power Syst. Res*, vol. 57, no. 1, pp. 41–48, Jan. 2001.

[12] K. Singh, N. P. Padhy, and J. Sharma, "Influence of price responsive demand shifting bidding on congestion and LMP in pool-based day-ahead electricity markets," *IEEE Trans. Power Syst*, vol. 26, no. 2, pp. 886–896, May 2011.

[13] D. Sun, "Experiences with LMP implementation," in *Proc. IEEE/Power Eng. Soc. General Meeting*, Jun. 18–22, 2006.

[14] D. Sun, "LMP and FTR in the standard market design," in *Proc. IEEE/Power Eng. Soc. Summer Meeting*, Jul. 25, 2002, vol. 3, pp. 1269–1270.

[15] [Online]. Available: http://ztuffaha.files.wordpress.com/2007/07/isone-difinitions.pdf.

[16] [Online]. Available: http://www.cirenew.info/pdfs/lmp.pdf.

[17] W. W. Hogan, Financial Transmission Right Formulations. [Online]. Available: http://whogan.com.

[18] V. Sarkar and S. A. Khaparde, "A comprehensive assessment of the evolution of financial transmission rights," *IEEE Trans. Power Syst*, vol. 23, no. 4, pp. 1783–1795, Nov. 2008.

[19] J. J. Grainger and W. D. Stevenson, Jr, *Power System Analysis*. New Delhi, India: Tata McGraw-Hill, 2003.

[20] California ISO, Market Optimization Details, Tech. Bull. 2009-06-05. Folsom, CA, CAISO, 2009.

[21] J. M. Arroyo and F. D. Galiana, "Energy and reserve pricing in security and network-constrained electricity markets," *IEEE Trans. Power Syst*, vol. 20, no. 2, pp. 634–643, May 2005.

[22] V. Sarkar and S. A. Khaparde, "Optimal LMP decomposition for the ACOPF calculation," *IEEE Trans. Power Syst*, vol. 26, no. 3, pp. 1714–1723, Aug. 2011.

Vaskar Sarkar received the Ph.D. degree from the Indian Institute of Technology, Bombay, India, in 2009.

He is an Assistant Professor of Electrical Engineering at Indian Institute of Technology, Hyderabad, India. His current research activities are in the areas of power system restructuring, high voltage dc transmission, smart grid, and microgrid.

S. A. Khaparde (M'87–SM'91) received the Ph.D. degree from the Indian Institute of Technology, Kharagpur, India, in 1981.

He is a Professor of electrical engineering at the Indian Institute of Technology, Bombay, India. His current research activities are in the areas of power system restructuring, distributed generation, and smart grid.